Journal of Organometallic Chemistry 716 (2012) 11–18

Contents lists available at SciVerse ScienceDirect

Journal of Organometallic Chemistry

journal homepage: www.elsevier.com/locate/jorganchem

A push–pull azobenzene is mercurated twice at the ring with less electron density

Philip J.W. Elder, Jeff C. Landry, Anthony F. Cozzolino, Allison E.A. Chapman, Ignacio Vargas-Baca*

Department of Chemistry and Chemical Biology, McMaster University, 1280 Main Street West, Hamilton, Ontario, Canada L8S 4M1

ARTICLE INFO

Article history:
Received 10 September 2011
Received in revised form
15 May 2012
Accepted 18 May 2012

Keywords:
Azodyes
Functionalization of azobenzenes
Mercuration
DFT calculations
Metallation reactions
Electrophilic substitution

ABSTRACT

Treatment of N,N-dialkyl-4-[4-nitrophenyl)diazenyl] anilines with a mercury(II) salt in anhydrous trifluoroacetic acid results in single and double metallation of the ring with less electron density. The seemingly counterintuitive outcome of the reaction was rationalized through experimental and computational investigations of the reaction mechanism.

1. Introduction

Driven to great extent by the search for pharmaceuticals and intermediates for organic synthesis, a vast variety of arylmercurials have been obtained in over 100 years of research [1–4]. The field has been recently reinvigorated by studies of the unique Lewis-acid properties of perfluorinated phenylmercurials. Their ability to form complexes with a variety of molecules [5,6], including conjugated alkynes [7], metallocenes [8], organic esters [9], and arenes [10] can be applied to the assembly of remarkable supramolecular structures [11–13]. Recent work has shown that mono- and di-functional Lewis acids containing bridging mercury atoms exhibit affinities for fluoride ions that rival those of their diboron counterparts, but possess greater stability in the presence of water [14]. Many of these species have been synthesized through transmetallation of the corresponding lithiated intermediates or Grignard reagents with mercuric salts (Eq. (1)); organomercury compounds can also be prepared by direct metallation (Eq. (2)). Activated aromatic molecules easily react with mercury(II) oxide, chloride, acetate or trifluoroacetate, in increasing order of reactivity [15].

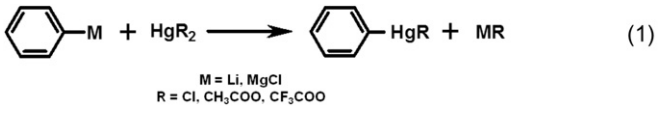

(1)

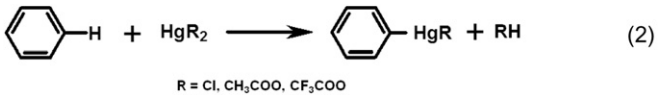

(2)

Direct mercuration of aromatic rings is strongly influenced by the nature of the substituent groups. Such effects are usually explicable by considering a classic electrophilic aromatic substitution (EAS) mechanism and the resonance of multiple canonical structures [16]; in the conventional formalism, electron-donating groups are *ortho*/*para* directors while electron-withdrawing groups are *meta*-directors. However, the reactions of mercuric salts with aromatic species occasionally yield results that – at first glance – are unexpected. For example, the mercuration of toluene exhibits a strong preference for *para*-substitution but equilibrium between all three possible isomers will ensue over long reaction times, especially in acidic medium [17]. This has been attributed to the ability of mercury in the arenemercurenium ions to shift when there is no kinetic control over the site of substitution [18]. The

* Corresponding author. Tel.: +1 905 525 9140; fax: +1 905 522 2509.
E-mail address: vargas@chemistry.mcmaster.ca (I. Vargas-Baca).

0022-328X/$ – see front matter © 2012 Elsevier B.V. All rights reserved.
http://dx.doi.org/10.1016/j.jorganchem.2012.05.040

low yield of *ortho*-mercurated products obtained from some monoalkyl-benzenes does suggest steric effects also impact these reactions [19]. Interestingly, while the mercuration of nitrobenzene yields predominantly *meta*-substituted species there is also a significant proportion of *ortho*-mercuration [20]. In general, substituents bearing electron lone pairs promote mercuration at the *ortho* position, which is usually assumed to be the consequence of an attractive interaction with the mercury ion [16].

The mercuration of larger molecules with extensively conjugated π-systems and a combination of donor and acceptor groups would be a convenient tool in the preparation of precursors for materials with a number of useful electronic and optical properties. However, the regiochemistry of such a reaction is difficult to predict because of the competition of different directing effects of several substituents, as is the case with the direct mercuration of diphenyl Schiff bases [21]. This issue greatly complicates the rational design of molecules of practical interest and efficient synthetic routes for their synthesis. In this context we examined the mercuration of push–pull azodyes, the N,N-dialkylamino, nitroazobenzenes **1** and **6**. The properties of such pseudostilbene chromophores have been studied in great detail due to their applicability in liquid crystals, electro-optical devices and nonlinear optical materials [22–27]. Preliminary results showed that the mercuration reaction occurs predominantly on the ring that – in principle – bears less electron density. Here we report the results of a combination of experimental and computational investigations that provide a rationale for our observations (Chart 1).

2. Experimental

2.1. Materials and methods

The manipulation of hygroscopic materials was performed under an atmosphere of anhydrous nitrogen with standard Schlenk and glovebox techniques. Trifluoroacetic acid was dehydrated by distillation over phosphorus pentoxide. All other reagents were used as received from Sigma–Aldrich (*p*-nitroaniline, ethyl aniline, *n*-pentanol), Caledon (potassium hydroxide), Fisher (lithium chloride), Baker (iodine), and Shawinigan (sodium nitrite). The silica gel used for column chromatography (EM Science) had a particle size of 40–63 μm.

Caution. Mercury and its compounds are toxic. They should be stored, handled and disposed of in a well-ventilated facility, wearing appropriate personal protective equipment and adhering to local safety, labour and environmental regulations.

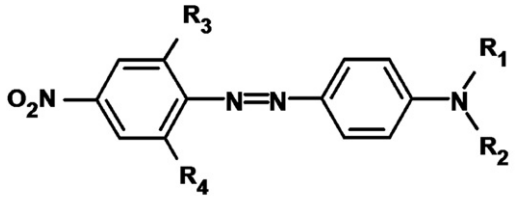

1 $R_1 = C_2H_5$; R_2 = n-C_5H_{11}; R_3, R_4 = H
2 $R_1 = C_2H_5$; R_2 = n-C_5H_{11}; R_3 = H; R_4 = HgCl
3 $R_1 = C_2H_5$; R_2 = n-C_5H_{11}; R_3, R_4 = HgCl
4 $R_1 = C_2H_5$; R_2 = n-C_5H_{11}; R_3 = H, R_4 = I
5 $R_1 = C_2H_5$; R_2 = n-C_5H_{11}; R_3, R_4 = I
6 R_1, $R_2 = CH_3$; R_3, R_4 = H
7 R_1, $R_2 = CH_3$; R_3 = H; R_4 = I

Chart 1.

Parallel syntheses were performed in a First-Mate Benchtop Synthesizer (Argonaut Technologies). HPLC analytical and semi-preparative runs were performed at room temperature on a Waters Spherisorb 5 μm ODS2 analytical column (4.6 × 150 mm, flow rate 2 mL min^{-1}) or a Waters Spherisorb S5 ODS2 semi-preparative column (10 × 250 mm, flow rate 8 mL min^{-1}) using the Waters 600E Multisolvent Delivery System (Waters 600 Controller, Waters 600E Pump). The separation was monitored with a Waters 2996 Photodiode Array Detector in conjunction with the Empower control software. Eluted fractions were recovered with a Waters Fraction Collector II and isolated with an Eppendorf 5301 Centrifugal Concentrator.

2.2. Spectroscopic instrumentation

^1H and $^{13}C\{^1H\}$ δ NMR spectra were acquired in solution on a Bruker DRX 500 (500.13 MHz) spectrometer; chemical shifts are reported in parts per million relative to tetramethylsilane (TMS) and were measured using the solvent as a secondary reference. $^{13}C\{^1H\}$ δ chemical shifts assignments were confirmed using 2-D techniques (HSQC and HMBC). Direct electron impact (DEI) mass spectra were obtained with a Micromass GCT (GC-EI/CI TOF) Mass Spectrometer. Infrared spectra were recorded on Bio-Rad FTS-40 spectrometer as KBr pellets. UV–visible spectra were obtained on a Cary 50 spectrophotometer. Melting points were recorded on a Thomas-Hoover capillary melting point apparatus and are reported uncorrected.

2.3. Syntheses

2.3.1. N-ethyl-N-pentyl aniline ($C_{13}H_{21}N$)

The aniline was prepared by a modification of a literature procedure [28]; using the alkyl iodide [29,30] in place of the bromide. A mixture of 1-iodopentane (20 mL, 0.153 mol) and N-ethyl-aminobenzene (13 mL, 0.103 mol) was added to potassium hydroxide (6.192 g, 0.110 mol) under nitrogen. The mixture was refluxed with stirring for 6 h, and the product was isolated as a clear, colourless liquid after distillation (68 °C, 0.4 torr). Yield: 15.03 g, 78.6 mmol, 76%. ^1H NMR (500 MHz, $CDCl_3$, 7.26 ppm): δ = 0.93 (t, 3H, H_{C19}), 1.16 (t, 3H, H_{C14}), 1.34 (m, 4H, H_{C17} H_{C18}), 1.60 (m, 2H, H_{C16}), 3.25 (t, 2H, H_{C15}), 3.38 (q, 2H, H_{C13}), 6.64 (m, 2H, H_{C3} H_{C8}), 6.68 (d, 2H, H_{C2} H_{C6}), 7.22 (t, 1H, H_{C7}). ^{13}C-DEPTq NMR (500 MHz, $CDCl_3$, 77.1 ppm): 12.4 (s, 1C, C14), 14.1 (s, 1C, C19), 22.7 (s, 1C, C17), 27.1 (s, 1C, C16), 29.5 (s, 1C, C18), 44.8 (s, 1C, C13), 50.4 (s, 1C, C15), 111.6 (s, 2C, C2 C6), 115.2 (s, 2C, C3 C5), 129.2 (s, 1C, C4), 147.9 (s, 1C, C1). HRMS (EI, %): *m*/*z* Found: 191.1679 (M^+, 15) Calculated 191.1674.

2.3.2. N-ethyl-4-[(4-nitrophenyl)diazenyl] N-pentylaniline ($C_{19}H_{23}N_4O_2$) (**1**)

The compound was prepared by azo coupling from *p*-nitroaniline (1.794 g, 13.0 mmol) and N-ethyl-N-pentyl aniline (2.502 g, 13.1 mmol) in 40 mL of 5 M HCl at 0 °C [31]. Sodium nitrite and acetate were used to remove excess NO_2 and neutralize the acid, respectively. A dark red solid was isolated by filtration and purified by column chromatography (100% $CHCl_3$). Yield: 3.888 g, 11.42 mmol, 88%. ^1H NMR (CD_2Cl_2): δ = 0.94 (t, 3H, H_{C19}), 1.25 (t, 3H, H_{C14}), 1.39 (m, 4H, H_{C17} H_{C18}), 1.67 (q, 2H, H_{C16}), 3.38 (t, 2H, H_{C15}), 3.51 (q, 2H, H_{C13}), 6.68 (d, 2H, H_{C2} H_{C6}), 7.93 (d, 2H, H_{C3} H_{C5}), 7.95 (d, 2H, H_{C8} H_{C12}), 8.31 (d, 2H, H_{C9} H_{C11}). ^{13}C-DEPTq NMR (500 MHz, CD_2Cl_2, 54.0 ppm): δ = 12.4 (s, 1C, C14), 14.1 (s, 1C, C19), 22.8 (s, 1C, C18), 27.4 (s, 1C, C16), 29.6 (s, 1C, C17), 45.6 (s, 1C, C13), 50.9 (s, 1C, C15), 111.6 (s, 2C, C2 C6), 122.8 (s, 2C, C8 C12), 125.1 (s, 2C, C9 C11), 126.7 (s, 2C, C3 C5), 143.6 (s, 1C, C4), 147.6 (s, 1C, C7), 152.3 (s, 1C, C1), 157.8 (s, 1C, C10). MP = 110–112 °C. UV (CH_2Cl_2): λ_{max} = 498 nm,

ε = 19,326 cm^2/mol. IR (cm^{-1}): 3732w, 3098w, 2951m, 2926m, 2869m, 1598s, 1584s, 1557m, 1515s, 1465w, 1455w, 1420w, 1404w, 1376s, 1360s, 1337s, 1307s, 1270s, 1254s, 1216m, 1189m, 1151m, 1139s, 1126s, 1102s, 1072m, 984w, 858m, 830m, 795w, 754w, 735w, 725w, 687w, 666w, 637w, 614w, 585w, 563w, 537w, 510w. HRMS (EI, %): *m*/*z* Found: 340.1906 (M^+, 13) Calculated 340.1899.

2.3.3. Mercuration of N-ethyl-4-[(4-nitrophenyl)diazenyl] N-pentylaniline

In a typical experiment, **1** (0.064 g, 0.19 mmol) and mercury trifluoroacetate (0.159 g, 3.72 mmol) were combined with anhydrous trifluoroacetic acid (0.13 mL) under nitrogen. The mixture was heated with stirring for 48 h in an oil bath at 68 °C. A concentrated solution of sodium chloride (0.055 g, 0.942 mmol) and sodium acetate (0.190 g, 2.31 mmol) was added to the reaction flask and the entire sample was treated with ultrasound for 10 min. The crude material was extracted with dichloromethane, dehydrated and used immediately for the iodination step.

2.3.4. Iodination of the mercuriated azodye

Iodine (0.202 g, 0.80 mmol) was added to the crude product of mercuration in chloroform. This solution was then stirred for 48 h and washed with concentrated sodium bicarbonate. Aqueous sodium thiosulfate was added to the mixture with stirring. After 5 min, the organic layer was separated and dehydrated with sodium sulfate then evaporated to dryness. The dark residue was treated with a mixture of acetonitrile–water (86% v/v) and separated by semi-preparative HPLC in 100 μL portions. The method employed an 8 mL/min flow rate with a stepwise elution profile that began isocratic 86% v/v for 14 min, and was followed by a linear gradient to 100% acetonitrile over 1 min. The two major fractions were collected, which were in order of elution:

(i) **N-ethyl-4-[(2,6-diiodo-4-nitrophenyl)diazenyl] N-pentylaniline** ($C_{19}H_{22}N_4O_2I_2$) (**5**). t_r = 12.4 min ^{1}H NMR (CD_2Cl_2): δ = 0.94 (t, 3H, H_{C19}), 1.25 (t, 3H, H_{C14}), 1.39 (m, 4H, H_{C17} H_{C18}), 1.69 (q, 2H, H_{C16}), 3.41 (t, 2H, H_{C15}), 3.51 (q, 2H, H_{C13}), 6.68 (d, 2H, H_{C2} H_{C6}), 7.91 (d, 2H, H_{C3} H_{C5}), 8.76 (s, 2H, H_{C9} H_{C11}). ^{13}C-DEPTq NMR (500 MHz, CD_2Cl_2, 54.0 ppm): δ = 12.6 (s, 1C, C14), 14.2 (s, 1C, C19), 23.0 (s, 1C, C18), 27.7 (s, 1C, C16), 29.9 (s, 1C, C17), 46.1 (s, 1C, C13), 51.4 (s, 1C, C15), 87.8 (s, 2C, C8 C12), 111.8 (s, 2C, C2 C6), 127.2 (s, 2C, C3 C5), 135.9 (s, 2C, C9 C11), 145.7 (s, 1C, C4), 147.0 (s, 1C, C7), 152.9 (s, 1C, C1), 159.4 (s, 1C, C10). UV (CH_2Cl_2): λ_{max} = 460 nm, ε = 13,080 cm^2/mol. IR (cm^{-1}): 3732w, 3363w, 3186w, 3088w, 3071w, 2957m, 2923s, 2852m, 1733w, 1646w, 1632w, 1605m, 1570w, 1556w, 1524w, 1508w, 1462w, 1410w, 1371w, 1333m, 1311w, 1275w, 1260w, 1216w, 1196w, 1184w, 1137m, 1114w, 1073w, 1043w, 995w, 946w, 914w, 893w, 879w, 822w, 795w, 749w, 739w, 720w, 703w, 525w, 503w. HRMS (EI, %): *m*/*z* Found: 591.9828 (M^+, 100) Calculated: 591.9832.

(ii) **N-ethyl-4-[(2-iodo-4-nitrophenyl)diazenyl] N-pentylaniline** ($C_{19}H_{23}N_4O_2I$) (**4**). t_r = 14.2 min ^{1}H NMR (CD_2Cl_2): δ = 0.94 (t, 3H, H_{C19}), 1.25 (t, 3H, H_{C14}), 1.39 (m, 4H, H_{C17} H_{C18}), 1.69 (q, 2H, H_{C16}), 3.41 (t, 2H, H_{C15}), 3.51 (q, 2H, H_{C13}), 6.82 (d, 2H, H_{C2} H_{C6}), 7.68 (d, 1H, H_{C12}), 7.94 (d, 2H, H_{C3} H_{C5}), 8.24 (dd, 1H, H_{C11}), 8.81 (d, 1H, H_{C9}). ^{13}C-DEPTq NMR (500 MHz, CD_2Cl_2, 54.0 ppm): δ = 12.7 (s, 1C, C14), 14.4 (s, 1C, C19), 23.1 (s, 1C, C18), 27.8 (s, 1C, C16), 29.8 (s, 1C, C17), 46.1 (s, 1C, C13), 51.4 (s, 1C, C15), 100.0 (s, 1C, C12), 112.0 (s, 2C, C2 C6), 117.5 (s, 1C, C8), 124.8 (s, 1C, C9), 127.7 (s, 2C, C5 C3), 135.4 (s, 1C, C11), 144.0 (s, 1C, C4), 147.7 (s, 1C, C7), 153.7 (s, 1C, C1), 156.3 (s, 1C, C10). UV (CH_2Cl_2): λ_{max} = 520 nm, ε = 27,310 cm^2/mol. IR (cm^{-1}): 3186w, 3086w, 2953m, 2921s, 2851m, 1734w, 1645w, 1600s, 1570m, 1555m, 1515s, 1436w, 1400m, 1357m, 1325s, 1314s, 1307s, 1262s, 1233s, 1196w, 1139s, 1104s, 1073m, 1024m, 992w, 892w, 869m, 834w, 818m, 798w, 747w, 727w, 691w, 634w, 566w, 539w, 518w. HRMS (EI, %): *m*/*z* Found: 466.0866 (M^+, 65) Calculated: 466.0866.

2.3.5. [(2-Iodo-4-nitrophenyl)diazenyl]N,N-dimethylaniline ($C_{14}H_{13}N_4O_2I$) (**6**)

The compound was prepared using the above mercuration method from 4-nitroaniline (1.02 g, 7.39 mmol) and N,N-dimethylaniline (0.887 g, 7.33 mmol), followed by mercuration of a small amount of material (0.0317 g, 0.117 mmol) with $Hg(CF_3CO_2)_2$ (0.120 g, 0.281 mmol) and treatment with iodine (0.203 g, 0.798 mmol), yielding a dark red powder (0.245 g, 0.906 mmol, 48%). Crystals suitable for X-ray diffraction were grown by slow evaporation of a chloroform/toluene solution. Yield = 1.616 g, 4.082 mmol, 56%. ^{1}H NMR (500 MHz, CD_2Cl_2, 5.32 ppm): δ = 3.13 (s, 6H, $N(CH_3)_2$), 6.78 (d, 2H, H2 H6), 7.66 (d, 2H, H9), 7.94 (d, 2H, H5 H3), 8.22 (dd, 2H, H8), 8.79 (d, 1H, H11). ^{13}C-DEPTq NMR (500 MHz, CD_2Cl_2, 54.0 ppm): 40.6 (s, 2C, $N(CH_3)_2$), 99.8 (s, 1C, C7), 112.2 (s, 2C, C2 C6), 117.5 (s, 1C, C8), 124.8 (s, 1C, C9), 127.4 (s, 2C, C3 C5), 135.4 (s, 1C, C11), 145.2 (s, 1C, C4), 148.4 (s, 1C, C12), 154.5 (s, 1C, C1), 156.0 (s, 1C, C10). UV (CH_2Cl_2): λ_{max} = 502 nm, ε = 25,294 cm^2/mol. IR (cm^{-1}): 3732w, 3087w, 2901w, 2854w, 2816w, 1610s, 1571m, 1553m, 1518s, 1506s, 1441w, 1416m, 1409m, 1357s, 1327s, 1306s, 1258m, 1238m, 1196w, 1139s, 1105s, 1064m, 1028w, 995w, 940w, 899w, 886w, 832w, 820m, 747w, 725w, 699w, 690w, 634w, 549w, 537w, 520w, 511w. HRMS (EI, %): *m*/*z* Found: 396.0094 (M^+, 100) Calculated: 396.0083.

2.4. Timed experiments

In a typical experiment, compound **1** (0.064 g, 0.19 mmol) and mercury trifluoroacetate (0.159 g, 3.72 mmol) were combined with anhydrous trifluoroacetic acid (0.13 mL) in each of six reaction tubes of a parallel synthesis reactor (Argonaut FirstMate™). The samples were maintained at 68 °C with vigorous stirring under nitrogen. Each mixture was quenched at a prescribed time by addition of 2 mL of a solution of sodium chloride (0.47 M) and sodium acetate (1.16 M). Each sample was treated with ultrasound for 10 min, washed repeatedly with aqueous sodium bicarbonate, centrifuged, and the supernatant was removed by pipette. The solid residue was treated with a solution of iodine in chloroform for 48 h. After removing the solvent, the solid samples were washed with aqueous sodium thiosulfate and water to remove residual iodine.

2.5. X-ray crystallography

A single crystal of **7** was mounted on a Siemens P4 four-cycle diffractometer with a Bruker 1000 CCD detector and a rotating anode utilizing Mo-Kα radiation (λ = 0.71073 Å, graphite monochromator) equipped with an OXFORD cryosystem. A hemisphere of reciprocal lattice was scanned in 0.36° steps in ω with a crystal-to-detector distance of 4.97 cm. Preliminary orientation matrices were obtained from the first frames using SMART [32]. The collected frames were integrated using preliminary orientation matrices which were updated every 100 frames. Final unit cell parameters were obtained by the refinement of the position of reflections with $I > 10\sigma(I)$ after integration of all data using SAINT [32]. The data sets were empirically corrected for absorption and other effects using SADABS [33]. The structure was solved by direct methods and refined by the full-matrix least squares method on all F^2 data using SHELXTL [34]. All non-H atoms were refined anisotropically; H atoms were constrained to idealized positions using

appropriate riding models. Molecular graphics were produced using Mercury (Version 2.3) [35].

2.6. Computational details

All structures were fully optimized using the ADF DFT package (versions 2007.01–2010.2) [36–38]. The adiabatic local density approximation (ALDA) was used for the exchange-correlation kernel [39,40], and the differentiated static LDA expression was used with the Vosko–Wilk–Nusair parameterizations [41]. The calculation of models of ground and transition state geometries was gradient-corrected with the exchange and correlation functionals of the gradient correction proposed in 1991 by Wang and Perdew [42,43]. Geometry optimizations were conducted using triple-ζ all-electron basis sets with one polarization function each and applying the zero order relativistic approximation (ZORA) [44] formalism with the specially adapted basis sets.

3. Results and discussion

Most of what is already known about the mercuration of azobenzenes derives from early studies which meticulously examined the reaction of the parent compound and several *ortho*-substituted derivatives [45]. In general, azobenzenes are not very reactive and do require stringent mercuration conditions. For example, 22 h of reflux in methanol with one equivalent of mercury acetate yields just 40% of *ortho*-monomercurated and 3% of each *o*,*o*- and *o*,*o*′ dimercurated products. Addition of a small amount of perchloric acid increases the corresponding yields to 55%, 8% and 9%. Similarly, reflux with mercury trifluoroacetate salt in neat trifluoroacetic acid yields 57% of *ortho*-monometallated product. The effect of the substituent groups is complicated. *Ortho*-methylazobenzene experiences 71% monomercuration on the substituted ring after 22 h of reflux in methanol with one equivalent of mercury acetate. *o*,*o*′-Dimethylazobenzene gives 51% monomercuration, and 4% *o*,*o*′-disubstitution under the same conditions, while *o*-methoxyazobenzene yields 63% monomercuration and 1% and 4% of *o*,*o*- and *o*,*o*′-dimercurials respectively [45]. Interestingly, electron-withdrawing groups in the *ortho* position appear to promote substitution of their own ring and noticeably decrease the yields (−I: 22%, $-NO_2$: 6%, −CN: 1%) of monomercurials. In most cases, the characterization/identification of the mercurated products is complicated by their limited solubility in common solvents; such a problem can be circumvented by working with the more soluble iodinated analogues. These are conveniently prepared by treatment of the organomercurials with elemental iodine; the reaction replaces the HgR group for an iodine atom without isomerization (Eq (3)) [45].

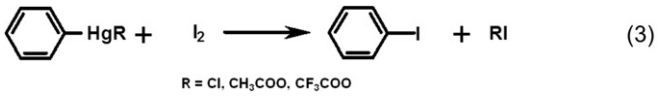

(3)

The observations summarized above do provide an excellent overview of the influence of individual substituents on the mercuration reaction of azobenzene but molecules that contain two substituents exerting competing effects, as would be the case of push–pull azobenzenes, are notably absent from that list. To fill in this gap, we conducted preliminary studies of the mercuration of the azodyes on [(4-nitrophenyl)diazenyl]N,N-dimethylaniline (**6**). Derivatization attempts with mercury (II) chloride and acetate were unsuccessful. Chromatographic evidence of partial mercuration of **6** was obtained with the trifluoroacetate in anhydrous trifluoroacetic acid [45]. However, the yield was low and the limited solubility of the product hampered optimization of the method. Longer alkyl groups were placed on the amino group in order to increase the solubility of the azodye. Satisfactory results were obtained for the N-ethyl-[(4-nitrophenyl)diazenyl] N-pentylaniline (**1**), therefore this compound was used for a full study of the reaction. After mercuration, the trifluoroacetate anion was exchanged for chloride in order to facilitate isolation of the products. The crude mercurated materials were usually obtained as dark-maroon solids which could not be thoroughly purified on their own because of their low solubility in common solvents. Instead, reaction with iodine in chloroform was used to produce the more soluble halogenated species; such a treatment indeed afforded a soluble material that was shown by NMR and HPLC to be a mixture. This analysis was accomplished using a custom HPLC separation method developed that combined gradient and isocratic water/acetonitrile regimes in analytical scale. Three major bands were observed, and the separation method was scaled up in order to collect samples large enough for spectroscopic characterization. Given the scale in which the purification could be efficiently carried out, identification of the components relied on NMR and mass spectrometry; combustion elemental analyses would have required large amounts of solvent, a bigger column and a higher throughput pump. Up to 7% of the material obtained from the iodination reaction eluted in 12 small fractions which could not be conclusively identified. Also from the chromatographic separation, 10% of starting material was recovered.

3.1. Structures of the isolated compounds

Each species was initially identified using two-dimensional ^1H NMR spectroscopy, taking advantage of the changes in the patterns of the aromatic region. The first band to elute ($t = 8.78$ min) corresponded to the unreacted azodye (**1**). Its NMR spectrum displays characteristic pairs of doublets of the amino [δ = 6.82, 7.93 ppm ($^3J_{H-H}$ = 9.02 Hz)] and nitro rings [δ = 7.95, 8.31 ppm ($^3J_{H-H}$ = 8.85 Hz)] with equal integrations. The second band (t = 12.37 min) belongs a di-substituted species giving three equally intense resonances in the aromatic region: two doublets at 6.68 ppm ($^3J_{H-H} = 9.11$ Hz) and 7.90 ppm ($^3J_{H-H} = 9.11$ Hz) which would belong to the amino ring and one singlet at 8.76 ppm which indicated that two iodine atoms are in equivalent positions, likely ortho to the azo bridge. The third band ($t = 14.21$ min) corresponds to a product of monosubstitution. While the chemical shifts of the protons in the amino ring are essentially unchanged [δ = 6.82, 7.94 ppm ($^3J_{H-H} = 9.00$ Hz)] the nitro ring protons produce two doublets at δ 7.68 ppm ($^3J_{H-H}$ = 9.00 Hz) and 8.81 ppm ($^3J_{H-H}$ = 2.52 Hz) which couple to the resonance centred at 8.24 ppm. On the basis of their ^1H NMR spectra the second and third major bands in the chromatogram were assigned to compounds **5** and **4** respectively (see Scheme 1 for ^1H NMR assignments).

3.2. X-ray crystallography

Although the NMR characterization of the species in the second band does show functionalization of the nitro ring, there remains

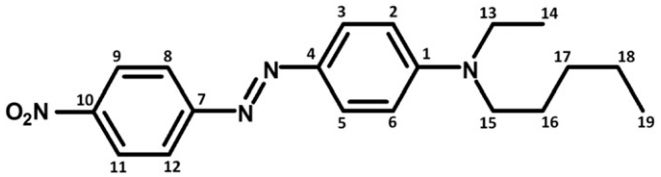

Scheme 1.

Table 1
Summary of crystal data, collection and refinement conditions for **7**.

	7
Formula	$C_{14}H_{13}N_4O_2I$
Formula weight	396.18
Radiation (wavelength, Å)	0.71073
Temperature	173 (2)
Crystal system	Monoclinic
Space group	I2/m
a (Å)	13.447 (4)
b (Å)	6.69 3(2)
c (Å)	16.799 (6)
α (°)	90.00
β (°)	99.083 (3)
γ (°)	90.00
Volume (Å^3)	1492.9 (8)
Z	4
$\delta_{calcd.}$ (g/cm^3)	1.763
m (mm^{-1})	2.155
R_1[a]	0.069
WR_2[b]	0.113

[a] $R_1 = \sum||F_o| - |F_c||/\sum|F_o|$.
[b] $WR_2 = (\sum w||F_o| - |F_c||^2/\sum w|F_o|^2)^{1/2}$.

ambiguity about the exact position of metallation. Both the nitro group and the azo bridge are known to have an ortho-directing effect. An assignment based only on the ^{1}H NMR chemical shifts would be uncertain because the aromatic protons are subject to both the inductive effect of the substituents and the anisotropic shielding from the π-electron cloud. Single-crystal X-ray diffraction would be the best way to make a definitive structural assignment. However, attempts to grow single crystals of the second band species were unsuccessful and only dendritic microcrystals were obtained. Instead the product of monosubstitution of **6** did yield crystals of good enough quality for structural determination. Data from the final refinement is provided in Table 1 (CCDC # 840135, included in supplementary). The structure of **7** (Fig. 1) does show the iodine atom *ortho*- to the azo bridge on the nitro-substituted ring. The molecule exhibits a perfectly planar structure, which is somewhat unexpected. Although there are no structurally characterized *ortho*-iodo azobenzenes, the structures of similarly *ortho*-halogenated azodyes [46] feature the halogenated ring rotated between 2.05° and 8.60° from the average plane and, in one notable extreme, 2′-bromo-4-(N-(2-cyanoethyl)-N-(2-phenylethyl)amino)-4′-nitroazobenzene has rings which are rotated 38.19° from each other [47]. The crystal structure of **7** does show displacement ellipsoids somewhat elongated along *b*. This fact suggests that there might be some disorder in the orientation of the rings with respect to each other and the observed flat structure might be the average; however, a satisfactory model for such a disorder could not be found. Despite these limitations, the structural determination did establish the position at which **6** underwent metallation. Given the similarities of their NMR spectra, **7** and the mono iodo derivative of **1** must have analogous connectivities, which confirms the identification of **4** as the species eluting at 14.2 min. This observation confirms by extension the identification of **5** and implies that the products of the mercuration reaction are **2** and **3**.

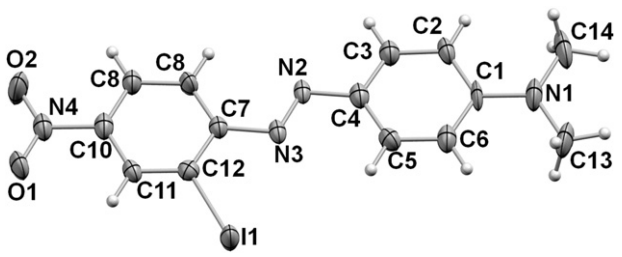

Fig. 1. ORTEP of 4-nitro, 2-iodo, 4-dimethylamino azobenzene, **7** (50% displacement ellipsoids). For clarity, all hydrogen atoms are displayed as spheres of ∅ = 0.15 Å. Selected bond lengths (Å) and angles (°): Avg. N4–O 1.212 (12), Avg. N1–C (methyl) 1.443 (16), N4–C10 1.474 (13), C8–I1 2.092 (10), C7–N3 1.426 (12), N3–N2 1.257 (11), N2–C4 1.382 (12), C1–N1 1.337 (12), O2–N4–C10 117.6 (9), C9–C8–I1 117.1 (7), C8–C7–N3 116.6 (9), C7–N3–N2 114.1 (8), N3–N2–C4 114.6 (9), N2–C4–C5 125.4 (9), C6–C1–N1 122.1 (11), C1–N1–C13 119.7 (10), C13–N1–C14 120.1 (10).

3.3. Temporal distribution of products

Once the ^{1}H NMR spectra of the predominant species were assigned, it became possible to use the 8.76 ppm singlet of **5**, the 8.81 ppm doublet of **4** and the 8.31 ppm doublet of **1** to probe the composition of the reaction mixture over time (after treatment of an aliquot with iodine). This method permitted an examination of the evolution of the system in the form of the plot presented in Fig. 2. The consumption of the monomercurated species to form the dimercurated product is only significant after an induction period of 2 h. However, the reaction does not appear to proceed to completion, with 10% of starting material remaining unreacted after 24 h. These features suggest that the mercuration steps might have a reversible character; alas the high concentrations and especially the formation of multiple by-products precluded the execution of a proper kinetic study in this case. In spite of the limitations, this information is useful to determine the reaction time that maximizes the yield of the monosubstituted species (Table 2).

3.4. Computational modelling

The most intriguing characteristic of the azodye mercuration process is the definite preference for reaction at the nitro-substituted ring. Invoking a conventional EAS mechanism, the reaction should occur on the amino-substituted ring because it is more electron rich. DFT calculations were carried out in an attempt to rationalize the experimental observations. In order to simplify modelling of the system, the calculations were performed on derivatives of the N,N-dimethyl dye, **6**, and chloride was used in lieu of the trifluoroacetate anion. The relative thermodynamic stabilities of all possible products of monomercuration were assessed by means of the comparison of the total bonding energies of their minimized structures; the result is graphically presented in Fig. 3. According to the DFT results, substitution at the positions *ortho* to the amino (C2, C6) and nitro (C9, C11) groups is less favourable than *ortho* to the azo bridge (C3, C5, C8, C12). There is little preference (<7 kJ/mol) for functionalization at C5 and C8 over C3 and C12 but overall the calculations do suggest there is no preference for reaction on either aromatic ring. Therefore, if the reaction were under thermodynamic control an approximately equimolar distribution of all the products of metallation *ortho* to the azo bridge would be obtained. Thermal rotation of the rings would exchange positions C3 and C5 as well as C8 and C12, but at least two isomer products of monometallation would be observed.

As the experimental observations appear to be in conflict with the thermodynamic preferences, attention was devoted to the reaction mechanism. In the initial stages of the reaction, the mercuric salt would dissociate, generating a HgX^+ cation which would add to the azodye, forming a transient species of general structure **8**. The most likely sites for electrophilic attack could be identified by the electrophilic Fukui function (Eq. (4)) [48,49], which is graphically approximated as the projection of the squared HOMO on the total electron density in Fig. 4. In this map, the darker areas indicate that the carbon atoms C2, C4, C6, C8, C10, and C12 are the most favourable points for an initial cation binding. However, steric repulsion would hinder substitution at C2 and C6; similarly C4 and C10 are unreactive because the nitro group and the azo

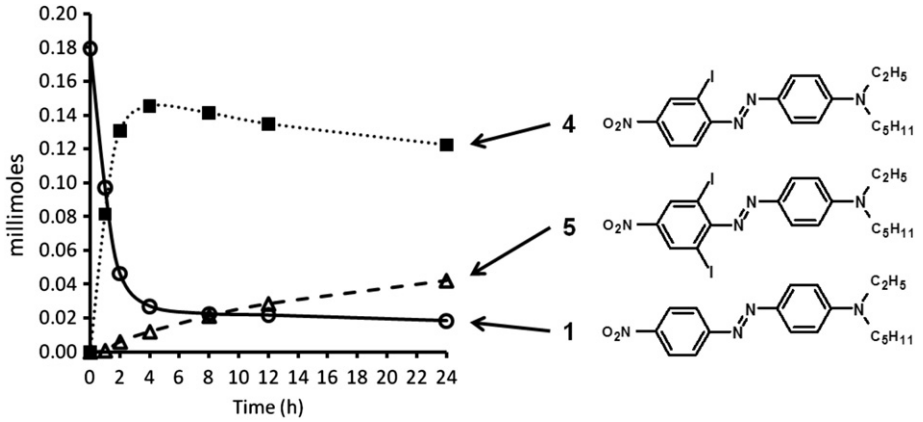

Fig. 2. Temporal evolution of the main components of the mixture used for mercuration and subsequent iodination of **1**. Spline lines highlight the trends but were not obtained by actual fitting to rate laws.

Table 2
Composition of the mixture used for mercuration and subsequent iodination of **1**.

Time (h)	Molar fractions		
	1	5	4
0	1.00	0.00	0.00
1	0.54	0.45	0.00
2	0.25	0.71	0.03
4	0.15	0.79	0.06
8	0.12	0.76	0.11
12	0.12	0.73	0.15
24	0.10	0.67	0.23

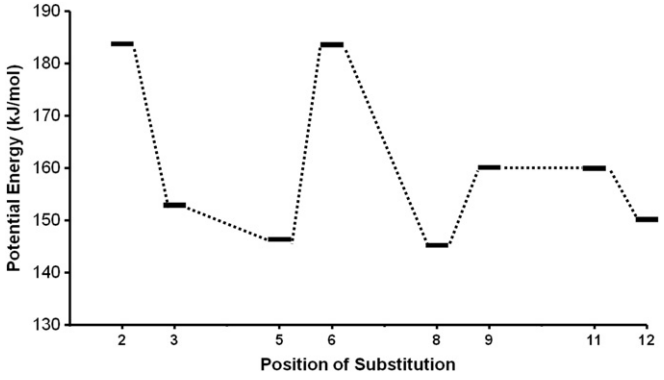

Fig. 3. Relative bonding energies of the possible products of metallation of **6**. (The carbon atoms and the positions of substitution are numbered as in Fig. 1.)

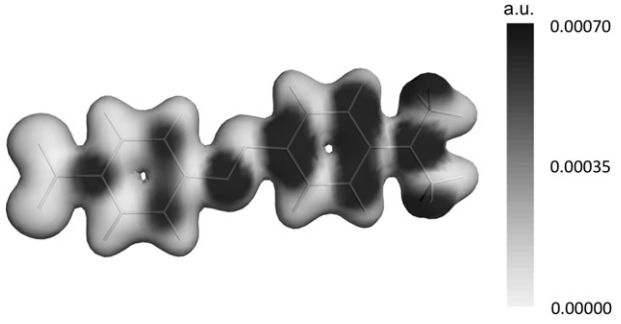

Fig. 4. Squared HOMO projected onto the total electron density of **6** (0.03 a.u. isosurface).

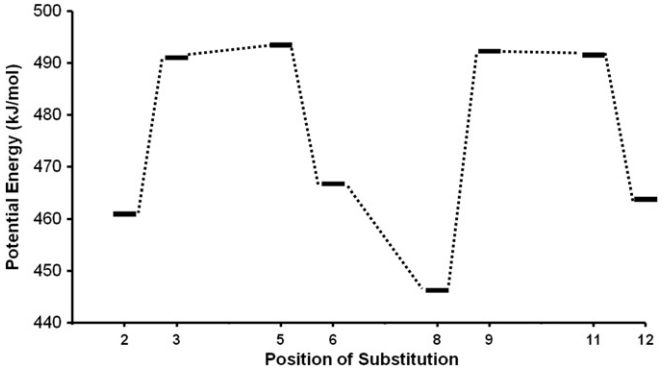

Fig. 5. Relative bonding energies of the transition states that would lead to each possible product of metallation. (The carbon atoms and the positions of substitution are numbered as in Fig. 1.)

bridge cannot be displaced. Although this result appears to agree with the experiment, a more rigorous analysis requires examination of the activation barrier. In this respect the mechanism of EAS reactions, including metallation, is suitable for quantum mechanical modelling because the barriers can be approximated by calculating the relative energies of **8**, which in most cases can be optimized [50–52]. In the present case, we calculated the geometries of the transition states which would lead to the substitution of each hydrogen on the aromatic rings. The relative energies of the structures are presented graphically in Fig. 5. In this case the results do show preference for the structure that would lead to metallation at C8, as experimentally observed. The next structure in order of energy is 14.7 kJ/mol above and would lead to mercuration at C2 (Chart 2).

$$f^{-}(r) = \rho_N(r) - \rho_{N-1}(r) \quad (4)$$

The results thus far discussed suggest that the substitution is directed by the combined effect of the substituents on reactivity of

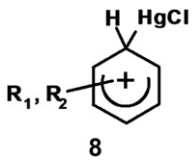

Chart 2.

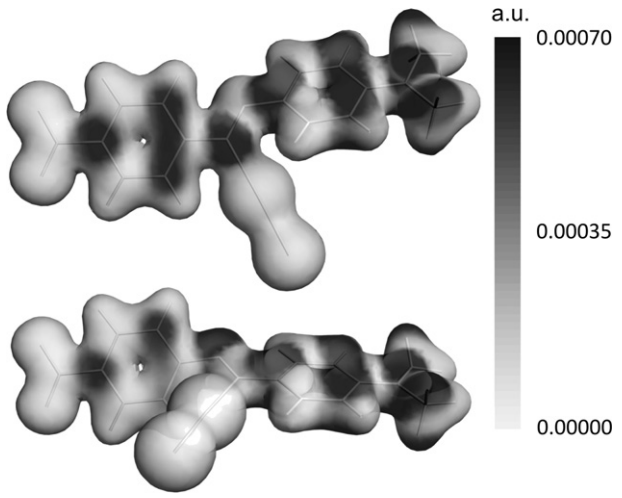

Fig. 6. Projections of the squared HOMOs onto the total electron densities (0.03 a.u. isosurfaces) of two isomers of $[Hg(Cl)(\mathbf{6})]^+$ coordinated by: a) N2 and b) N3.

each carbon. However, it has been suggested that the azo bridge itself may play an active role in the mercuration mechanism as the initial point of cation binding, from which HgX^+ would migrate onto the position of substitution [45]. Indeed the map of the electrophilic Fukui function of **6** (Fig. 4) identifies the bridge as a reactive site but only through N3, which is *ortho* to the position of actual substitution. The effect of attachment of the cation on the reactivity of the carbon atoms was then investigated with the maps of the electrophilic Fukui function on optimized models of **6** binding $[HgCl]^+$ by N3 and, for comparison, N2 (Fig. 6). In both instances binding to the azo bridge causes rotation of the aromatic rings, to interplanar angles greater than 55°; in each case, the mercury atom is in the plane of the adjacent benzene. The electrophilic Fukui functions of the mercury bound **6** show little change with respect to the free molecules, i.e. the reactivity of the C atoms is preserved, this also suggests that mercury migration and substitution would preferentially happen onto C8 and C12, in agreement with the experiment.

4. Summary and outlook

The combination of electron donating and withdrawing groups reduces the reactivity of azobenzene towards direct mercuration, thus very aggressive conditions such as mercury(II) trifluoroacetate in anhydrous trifluoroacetic acid are necessary to achieve the functionalization of the chromophore. Even then, the reaction does not proceed quantitatively, leaving behind a significant proportion of starting material. The two major products are the result of sequential metallation of the nitro-substituted ring, at the positions ortho to the azo bridge. The DFT study of the reagent and models of the possible isomers of the first product and the corresponding transition states points to a system under kinetic control and the electrophilic Fukui function correctly identifies the most reactive positions. The results and methods of this study constitute a tool for the preparation of intermediates in the synthesis of functional molecules and materials derivatized with organic chromophores.

Acknowledgements

This project was supported by grants from the Natural Sciences and Engineering Research Council of Canada (NSERC), the Canada Foundation for Innovation (CFI), and the Ontario Innovation Trust (OIT). This work was made possible by the facilities of the Shared Hierarchical Academic Research Computing Network (SHARCNET: www.sharcnet.ca).

Appendix A. Supplementary material

CCDC # 840135 contains the supplementary crystallographic data for this paper. These data can be obtained free of charge from The Cambridge Crystallographic Data Centre via www.ccdc.cam.ac.uk/data_request/cif.

Appendix B. Supplementary material

Supplementary material associated with this article can be found, in the online version, at http://dx.doi.org/10.1016/j.jorganchem.2012.05.040.

References

[1] N.N. Greenwood, A. Earnshaw, Chemistry of the Elements, second ed. Butterworth Heinemann, Oxford, 1997, pp. 1222–1224.
[2] G.E. Coates, Organometallic Compounds, Wiley, London, 1960, pp. 72–87.
[3] R.C. Larock, Organomercury Compounds in Organic Synthesis, Springer-Verlag, New York, 1985.
[4] J.L. Wardell, Mercury, in: G. Wilkinson, F.G.A. Stone, E.W. Abel (Eds.), Comprehensive Organometallic Chemistry, vol. 2, Pergamon Press Ltd., Toronto, 1982, pp. 863–978.
[5] M. Tschinkl, A. Schier, J. Riede, F.P. Gabbaï, Organometallics 18 (1999) 2040–2042.
[6] M. Tschinkl, F.P. Gabbaï, J. Chem. Crystallogr. 33 (2003) 595–598.
[7] T. Taylor, O. Elbjeirami, C. Burress, M. Tsunoda, M. Bodine, M. Omary, F.P. Gabbaï, J. Inorg. Organomet. Polym. 18 (2008) 175–179.
[8] M.R. Haneline, F.P. Gabbaï, Angew. Chem. Int. Ed. 43 (2004) 5471–5474.
[9] A.A. Yakovenko, J.H. Gallegos, M.Y. Antipin, A. Masunov, T.V. Timofeeva, Cryst. Growth Des. 11 (2011) 3964–3978.
[10] T.J. Taylor, C.N. Burress, L. Pandey, F.P. Gabbaï, Dalton Trans. (2006) 4654–4656.
[11] T.J. Taylor, C.N. Burress, F.P. Gabbaï, Organometallics 26 (2007) 5252–5263.
[12] G.B. Deacon, C.M. Forsyth, P.C. Junk, E.I. Izgorodina, T.J. Ness, G. Meyer, I. Pantenburg, CrystEngComm 13 (2011) 88–92.
[13] G.B. Deacon, C.M. Forsyth, P.C. Junk, T.J. Ness, E. Izgorodina, J. Baldamus, G. Meyer, I. Pantenburg, J. Hitzbleck, K. Ruhlandt-Senge, Eur. J. Inorg. Chem. (2008) 4770–4780.
[14] C.L. Dorsey, P. Jewula, T.W. Hudnall, J.D. Hoefelmeyer, T.J. Taylor, N.R. Honesty, C.-W. Chiu, M. Schulte, F.P. Gabbaï, Dalton Trans. (2008) 4442–4450.
[15] K.A. Kobe, T.F. Doumani, Ind. Eng. Chem. 33 (1941) 170–176.
[16] Y. Ogata, M. Tsuchida, J. Org. Chem. 20 (1955) 1637–1643.
[17] H.C. Brown, C.W. McGary, J. Am. Chem. Soc. 77 (1955) 2300.
[18] G.A. Olah, I. Hashimoto, H.C. Lin, Proc. Natl. Acad. Sci. U.S.A. 74 (1977) 4121.
[19] H.C. Brown, C.W. McGary, J. Am. Chem. Soc. 77 (1955) 2310–2312.
[20] Y. Ogata, M. Tsuchida, J. Org. Chem. 20 (1955) 1644–1649.
[21] H.B. Singh, W.R. McWhinnie, J. Chem. Soc. Dalton Trans. (1985) 821.
[22] Z. Li, W. Wu, Q. Li, Y. Gui, L. Xiao, Y. Liu, C. Ye, J. Qin, Z. Li, Angew. Chem. Int. Ed. 49 (2010) 2763.
[23] J. Garcia-Amorós, H. Finkelmann, D. Velasco, Chem. Eur. J. 17 (2003) 6518.
[24] A.G. Chen, D.J. Brady, Appl. Phys. Lett. 62 (1993) 2920.
[25] M. Lee, H.E. Katz, C. Erben, D.M. Gill, P. Gopalan, J.D. Heber, D.J. McGee, Science 298 (2002) 1401.
[26] P. Gopalan, H.E. Katz, D.J. McGee, C. Erben, T. Zielinski, D. Bousquet, D. Muller, J. Grazul, V. Olsson, J. Am. Chem. Soc. 126 (2004) 1741–1747.
[27] M.M.M. Raposo, M.C.R. Castro, A.M.C. Fonseca, P. Schellenberg, M. Belsley, 67 (2011) 5189–5198.
[28] A.R. Lepley, W.A. Khan, J. Org. Chem. 33 (1968) 4362–4368.
[29] E.C. Ashby, J. Oswald, J. Org. Chem. 53 (1988) 6068–6076.
[30] H. Finkelstein, Chem. Ber. 43 (1910) 1528–1532.
[31] A.I. Vogel, A Textbook of Practical Organic Chemistry, Longman, London, 1957, p. 1188.
[32] SMART and SAINT, Siemens Analytical X-ray Instruments Inc, Madison, Wisconsin, USA, 1995.
[33] SADABS, Bruker AXS Inc., Madison, Wisconsin, USA, 2001.
[34] (a) G.M. Sheldrick, SHELX97 [Includes SHELXS97, SHELXL97, CIFTAB]. Programs for Crystal Structure Analysis. Release 97-2, Institüt für Anorganische Chemie der Universität, Göttingen, Germany, 1997;
(b) G.M. Sheldrick, Acta Crystallogr. A64 (2008) 112–122.
[35] C.F. Macrae, I.J. Bruno, J.A. Chisholm, P.R. Edgington, P. McCabe, E. Pidcock, L. Rodriguez-Monge, R. Taylor, J. van de Streek, P.A. Wood, J. Appl. Crystallogr. 41 (2008) 466–470.
[36] G. te Velde, F.M. Bickelhaupt, E.J. Baerends, C. Fonseca Guerra, S.J. A. van Gisbergen, J.G. Snijders, T. Ziegler, J. Comput. Chem. 22 (2002) 931–967.
[37] C. Fonseca Guerra, J.G. Snijders, G. te Velde, E.J. Baerends, Theor. Chem. Acc. 99 (1998) 391–403.
[38] E.J. Baerends, J. Autschbach, A. Bérces, C. Bo, P.M. Boerrigter, L. Cavallo, D.P. Chong, L. Deng, R.M. Dickson, D.E. Ellis, M. van Faassen, L. Fan, T.H. Fischer, C.F.

Fonseca Guerra, S.J.A. van Gisbergen, J.A. Groeneveld, O.V.Gritsenko, M. Grüning, F.E. Harris, P. van der Hoek, H. Jacobsen, G. Jensen, G. van Kessel, F. Kootstra, E. van Lenthe, D.A. McCormack, A. Michalak, V.P. Osinga, S. Patchkovskii, P.H.T. Philipsen, D. Post, C.C. Pye, W. Ravenek, P. Ros, P.R.T. Schipper, H.G. Schreckenbach, J.G. Snijders, M. Solà, M. Swart, D. Swerhone, G. te Velde, P. Vernooijs, L. Versluis, O. Visser, F. Wang, E. van Wezenbeek, G. Wiesenekker, S.K. Wolff, T.K. Woo, T. Ziegler, ADF 2010.01, 2010.
[39] S.J.A. van Gisbergen, J.G. Snijders, E.J. Baerends, Phys. Rev. Lett. 78 (1997) 3097–3100.
[40] S.J.A. van Gisbergen, J.G. Snijders, E.J. Baerends, J. Chem. Phys. 109 (1998) 10644–10656.
[41] S.H. Vosko, L. Wilk, M. Nusair, Can. J. Phys. 58 (1980) 1200–1211.
[42] J.P. Perdew, Phys. Rev. B 33 (1986) 8822–8824.
[43] J.P. Perdew, Y. Wang, Phys. Rev. B 45 (1992) 13244–13249.
[44] E. van Lenthe, A. Ehlers, E.J. Baerends, J. Chem. Phys. 110 (1999) 8943–8953.
[45] P.V. Roling, D.D. Kirt, J.L. Dill, S. Hall, C. Hollstrom, J. Organomet. Chem. 116 (1976) 39–53.
[46] X.-L. You, Y. Zhang, Y. Zhang, D.-C. Zhang, Acta Crystallogr. Sect. E. Struct. Rep. Online 61 (2005) o2656–o2658.
[47] M.L. Glowka, Z. Olubek, Acta Crystallogr. C. Cryst. Struct. Commun. 50 (1994) 458–460.
[48] W. Yang, R.G. Parr, R. Pucci, J. Chem. Phys. 81 (1984) 2862–2863.
[49] R.G. Parr, W. Yang, J. Am. Chem. Soc. 106 (1984) 4049–4050.
[50] S. Kolboe, S. Svelle, B. Arstad, J. Phys. Chem. A 113 (2009) 917–923.
[51] S. Kolboe, J. Phys. Chem. A 115 (2011) 3106–3115.
[52] J.S. Kadavalli, D.R. Boyd, D. Coyne, J.R. Keeffe, D.A. Lawlor, A.C. MacCormac, R.A.M. O'Ferrall, S.N. Rao, N.D. Sharma, Org. Lett. 12 (2010) 5550–5553.